NASA TECHNICAL NOTE

NASA TN D-4291

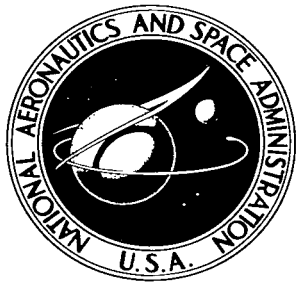

NASA TN D-4291

BALLISTIC-RANGE TESTS OF A DRAG-RING CONFIGURATION AT MACH NUMBERS AROUND 2

by Charles E. DeRose

Ames Research Center
Moffett Field, Calif.

NATIONAL AERONAUTICS AND SPACE ADMINISTRATION • WASHINGTON, D. C. • DECEMBER 1967

BALLISTIC-RANGE TESTS OF A DRAG-RING CONFIGURATION AT MACH NUMBERS AROUND 2

By Charles E. DeRose

Ames Research Center
Moffett Field, Calif.

NATIONAL AERONAUTICS AND SPACE ADMINISTRATION

For sale by the Clearinghouse for Federal Scientific and Technical Information
Springfield, Virginia 22151 – CFSTI price $3.00

BALLISTIC-RANGE TESTS OF A DRAG-RING CONFIGURATION AT MACH NUMBERS AROUND 2

By Charles E. DeRose

Ames Research Center

SUMMARY

Free-flight measurements of an unusual configuration proposed as a Mars atmospheric probe were made in the Ames Pressurized Ballistic Range. The configuration consisted of a cone-cylinder centerbody supported within a large conical-sector flare (called a drag ring) with a wide gap between the two components. Tests were made in air at a nominal Mach number of 2 and a Reynolds number, based on the drag-ring diameter of 50,000. All experimental data are compared with values obtained at a Mach number of 20 and with Newtonian theory to check the effect of a large change in flight velocity.

The drag coefficient of this shape decreased from 1.2 at 0° angle of attack to 0.95 at 12° angle of attack.

Values of lift-curve slope and pitching-moment-curve slope at Mach number 2 were in fair agreement with those at Mach number 20, suggesting that these derivatives may not vary with flight Mach number. These two derivatives were also constant with angle of attack for these test conditions, which included pitching amplitudes from 2° to 15°.

The damping derivatives indicated dynamic stability at Mach numbers under 2, but one flight at Mach number 2.4 was dynamically unstable. The change in flow about the drag ring with velocity is believed to have caused the change in damping.

Flow-visualization photographs show essentially choked flow between the drag ring and the centerbody for all flights, and the bow-shock wave was outside the drag ring except at $M = 2.4$. The outward movement of the bow-shock wave was caused by the separation of flow over the nose cone.

INTRODUCTION

In seeking an optimum configuration for an unmanned probe to measure atmospheric properties on neighboring planets, the designer is immediately faced with two conflicting requirements: first, the desire for a high-drag shape to extend the time for making measurements; and, second, the need to overcome communication blackout, which usually means adopting a sharp, low-drag nose. The Martin Company, in a proposal for an atmospheric probe for Mars, designed a unique configuration that satisfies both of these design

requirements. Basically, the configuration consists of a sharp, cone-cylinder centerbody supported by cruciform struts within a short annular drag ring (fig. 1).

Preliminary theoretical and wind-tunnel force test studies (by S. M. Gottlieb, D. S. Szelo, and H. C. Norman of The Martin Co.) fixed the shape of the configuration and showed aerodynamic coefficients to be well predicted by Newtonian theory at $M = 20$ in air at high enthalpies. To evaluate the configuration over a broad velocity range, static- and dynamic-stability data were needed at lower Mach numbers. There was speculation that nonlinearities in the aerodynamic derivatives might occur at Mach numbers between 2 and 3 when the bow-shock wave theoretically starts to impinge on the leading edge of the drag ring.

A limited investigation was undertaken in the Pressurized Ballistic Range at Ames Research Center to study the drag, lift, and static and dynamic stability of this shape in air at a Mach number of approximately 2, and to photograph the flow around the free-flying model. The results of this investigation are reported here.

The models used for this test program were designed and constructed by The Martin Company, Denver Division, whose assistance in this phase of the investigation is greatly appreciated.

SYMBOLS

A	reference area, $\frac{\pi D^2}{4}$, m^2
C_D	drag coefficient, $\frac{\text{drag}}{(1/2)\rho V^2 A}$, dimensionless
C_L	lift coefficient, $\frac{\text{lift}}{(1/2)\rho V^2 A}$, dimensionless
C_{L_σ}	lift-curve slope, $\frac{\partial C_L}{\partial \sigma}$, per radian
C_m	pitching-moment coefficient, $\frac{\text{pitching moment}}{(1/2)\rho V^2 AD}$, dimensionless
C_{m_σ}	pitching-moment-curve slope, $\frac{\partial C_m}{\partial \sigma}$, per radian
$(C_{m_q}+C_{m_{\dot{\alpha}}})$	damping-in-pitch derivative, $\frac{\partial C_m}{\partial \dot{\theta}(D/V)} + \frac{\partial C_m}{\partial \dot{\alpha}(D/V)}$
D	reference diameter, diameter of base of drag ring, m
M	Mach number

R	Reynolds number based on drag-ring diameter and free-stream conditions
V	velocity along flight path, m/sec
X_{cg}	axial distance from base of model to center of gravity, m
α	angle of attack (in vertical plane), deg
β	angle of sideslip (in horizontal plane), deg
σ	resultant angle of attack, $\tan^{-1}\sqrt{(\tan\alpha)^2 + (\tan\beta)^2}$, deg
ρ	free-stream air density, kg/m^3
$(\ )_{rms}$	root mean square $\sqrt{\frac{\int_0^x (\ )^2\, dx}{x}}$

FACILITY, MODELS, AND TECHNIQUES

The Ames Pressurized Ballistic Range is a variable pressure facility with 24 spark shadowgraph stations along a 62-meter instrumented length. Each station takes a pair of orthogonal spark-illuminated shadowgraphs. The models were launched from a 57-mm smooth-bore gun into still air at a pressure of 0.02 atm and a velocity from 600 to 800 m/sec.

The models were constructed of 2024 aluminum with a bronze nose to fix the center of gravity at the design point (see figs. 1 and 2). The upper struts, drag ring, and aft section of the body were machines from a solid piece of material. The lower struts were soldered to the body and drag ring after being machined. The bronze nose was fastened to the body with a threaded stud.

Because of the very light weight and high drag of the model, the sabot had to be mechanically decelerated and removed at the muzzle of the gun. This was accomplished by passing the model and sabot through a 51.5 mm diameter hole in a steel plate. The model passed through freely, but the sabot (57 mm diameter) was slowed down by the shearing off of its outer 2.7 mm.

The sabot was constructed in three parts (fig. 3): the main body (foamed-in-place polyurethane plastic), a model-support pedestal (Lexan), and a rear shear disk (Lexan). The main body, cast to size and shape from foamed-in-place plastic in a nominally sealed mold, had an average specific gravity of 0.25. However, the density of the hardened sabot was not uniform; the walls were dense and the center was very porous (fig. 4). This result was advantageous: when the sabot sheared through the decelerating plate, the strong outer wall was removed, allowing aerodynamic forces to shred away the remaining sabot body. Figure 5 shows the sabot after passing through the decelerating plate.

ANALYSIS OF DATA

The data in this report are from analyses of the time histories of the model motion as obtained from the 24 sets of orthogonal shadowgraphs, with the time reference obtained from 1.6 MHz chronographs.

A detailed description of the specific method of data reduction can be found in reference 1.

RESULTS AND DISCUSSION

The data are presented in figures 6 to 9 and compared with results from the Martin 24-inch arc-heated, blow-down wind tunnel obtained at Mach number 20 and with values from Newtonian theory ($C_{p_{max}} = 2$). The conditions for the serially numbered tests are presented in table I.

TABLE I.- FLIGHT TEST CONDITIONS AND RESULTS

Flight	Range pressure, atm	Mach no.	Reynolds no.	σ_{rms}, deg	C_D	C_{L_σ}	C_{m_σ} (measured)	C_{m_σ} (X_{cg} = 26.7 percent D)	$C_{m_q} + C_{m_{\dot{\alpha}}}$
1	0.01912	1.989	44,783	3.104	1.091	---	---	---	---
2	.01912	1.874	42,199	14,497	.923	-0.384	-0.212	-0.218	-0.602
3	.02047	2.396	57,996	9.070	.980	-.455	-.207	-.215	---
4	.02099	1.638	40,751	2.520	1.124	---	-.225	-.225	-.472
5	.01912	2.358	52,244	10.480	.969	-.465	-.212	-.212	.179

Figure 6 shows the drag coefficient as a function of root-mean-squared resultant angle of attack. Since the Mach number range was limited, no attempt was made to obtain a variation of C_D with this variable. As can be seen, the drag coefficient varied from approximately 1.2 at 0° angle of attack to about 0.95 at a root-mean-squared angle of attack of 12°.

In figure 7, C_{L_σ} is plotted as a function of root-mean-squared resultant angle of attack for the three tests in which the model swerved sufficiently to permit measurements. The free-flight data at M = 2 agree reasonably well with M = 20 data, suggesting that Mach number has little effect on this derivative. It is also seen that C_{L_σ} does not appear to be a strong function of angle of attack over the test range.

The pitching-moment-curve slope, C_{m_σ}, is shown in figure 8 as a function of angle of attack. Data are presented for all tests long enough to permit accurate determination of wavelength. All results shown are adjusted to a common center of gravity (X_{cg} is 26.7 percent of the base diameter). The adjustment, in all cases, was less than 7 percent. As shown in figure 8, C_{m_σ} is constant up to an angle of attack of 14° (i.e., linear aerodynamic properties). These values of the static-stability derivative are also seen to be close to those at M = 20, again suggesting that Mach number has little effect on this aerodynamic parameter.

The damping derivative ($C_{m_q} + C_{m_{\dot{\alpha}}}$) could be determined only for those tests with at least three peaks in the angle-time history. The three values obtained are shown in figure 9. The two flights at the lower Mach numbers show stable damping (negative values of $C_{m_q} + C_{m_{\dot{\alpha}}}$); and the one flight at higher Mach number shows unstable damping. The change in velocity could be responsible for this change in damping because it alters the flow through the drag ring. As can be seen in the shadowgraphs in figure 10, the flow is separated from the nose in all cases. However, as the Mach number is changed from 1.8 to 2.3, the angle of the separated flow decreases rapidly, allowing a partial unchoking of the flow on the windward side at the higher Mach number, which might not be possible at the lower Mach number. The effect of this variable flow with angle of attack at the higher Mach number might cause the change in damping derivative; on the other hand, this variation in flow does not affect the static-stability results.

The three tests used to obtain the damping derivatives are further described in figure 11, which shows the degree of fit between the motion calculated by the deduced aerodynamic coefficients and the experimentally observed angles. Flights 2 and 5 show relatively good agreement but flight 4 appears less accurate because of the small amplitude. It should be noted that all motions are reasonably planar, a condition that affords good damping data.

CONCLUSIONS

The flared ring and stabilized cone-cylinder proposed by The Martin Company for a Mars atmospheric probe has been tested in free flight in air at Mach numbers around 2 and Reynolds numbers near 50,000. The static aerodynamic results of the present test are similar to those obtained at $M = 20$ in an arc-heated wind tunnel. The dynamic-stability results show that for two flights below $M = 2$ oscillations converged and for one flight above $M = 2$ oscillations diverged slightly. The change in damping coincided with changes in the flow structure over the centerbody and through the drag ring.

Ames Research Center
National Aeronautics and Space Administration
Moffett Field, Calif., 94035, Oct. 4, 1967
124-07-02-35-00-21

REFERENCE

1. Intrieri, Peter F.: Effects of Transverse Center-of-Gravity Displacement, Afterbody Geometry, and Front-Face Curvature on the Aerodynamic Characteristics of Mercury-Type Models at a Mach Number of 5.5. NASA TM X-569, 1961.

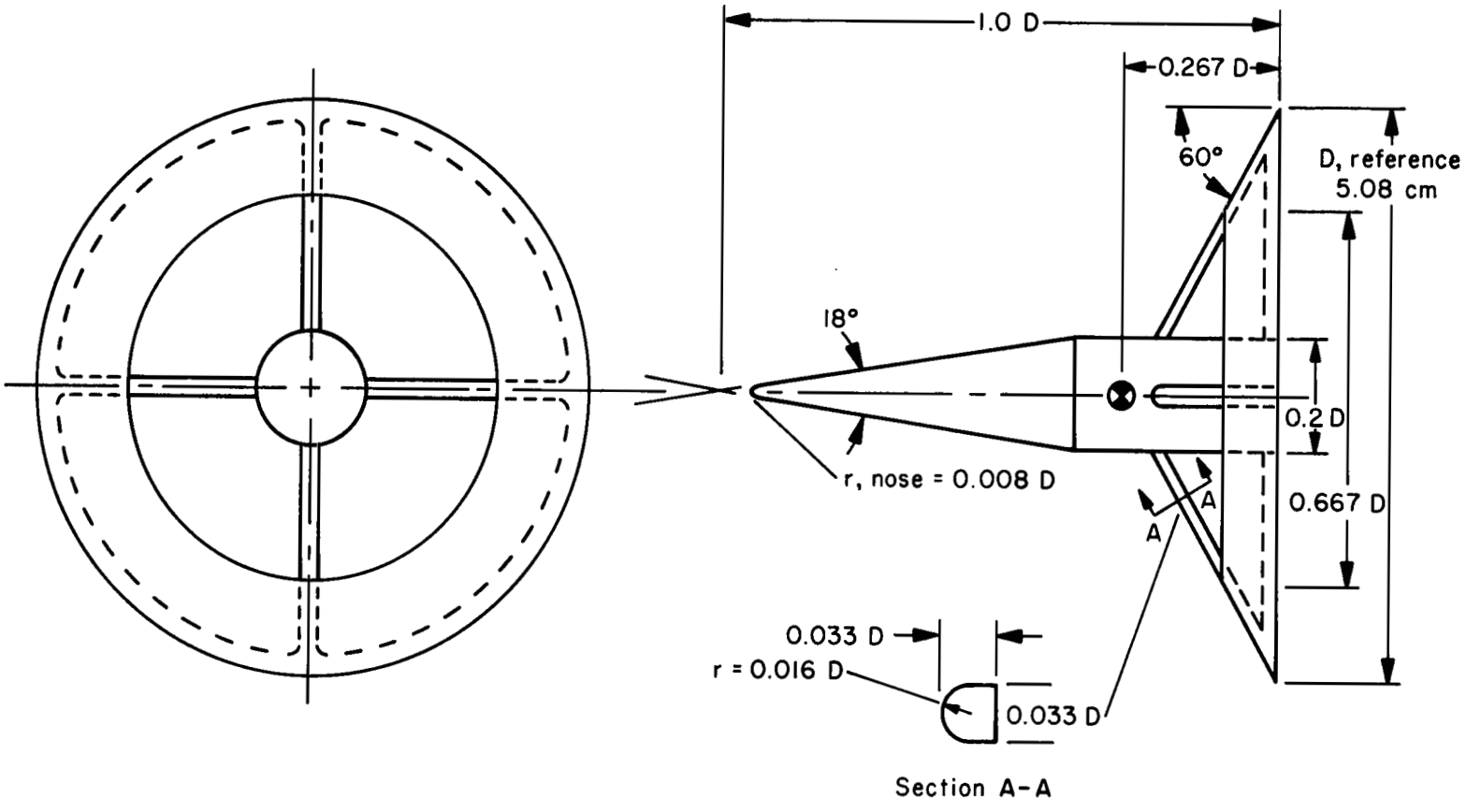

Figure 1.- Drag-ring model.

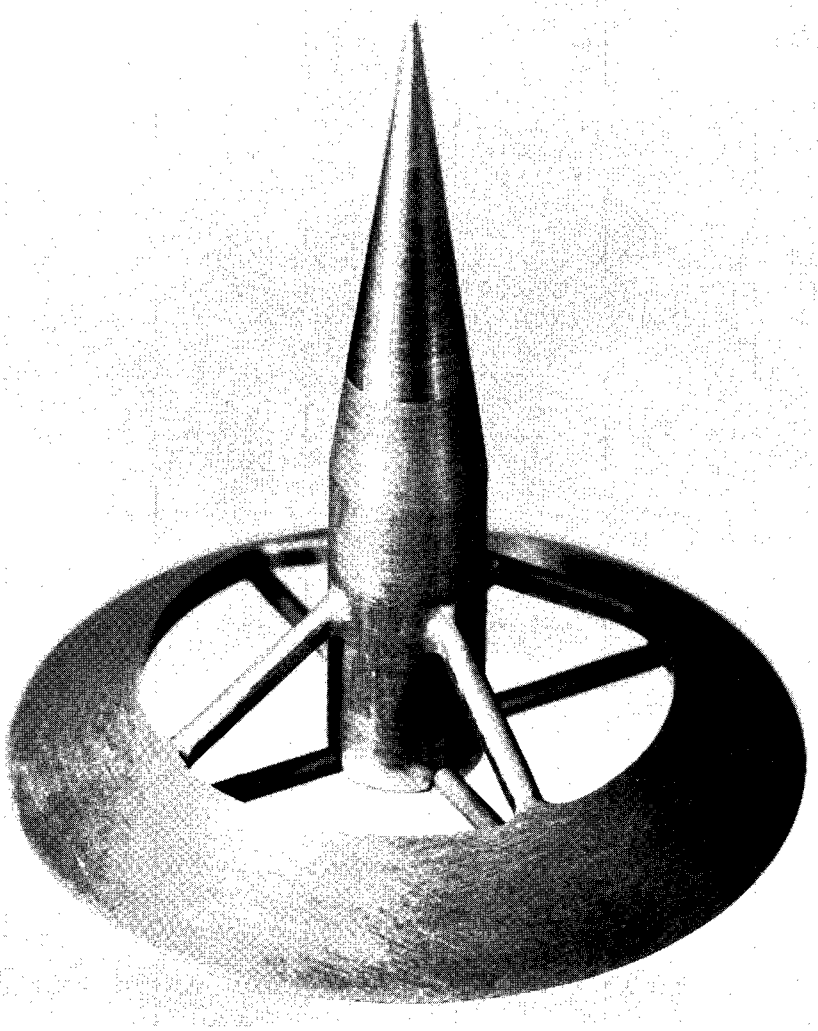

A-37388

Figure 2.- Model.

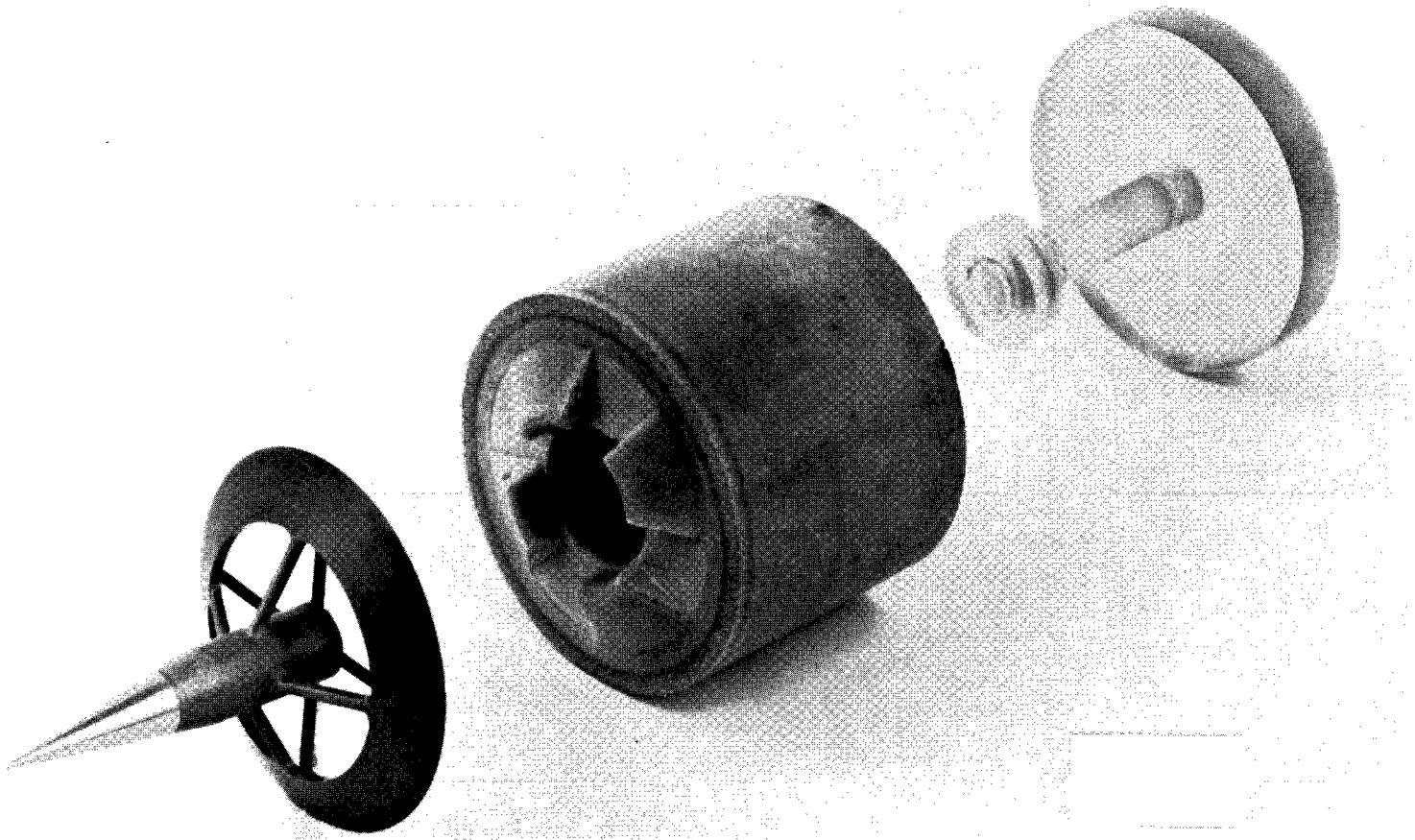

A-37389

Figure 3.- Model and sabot combination.

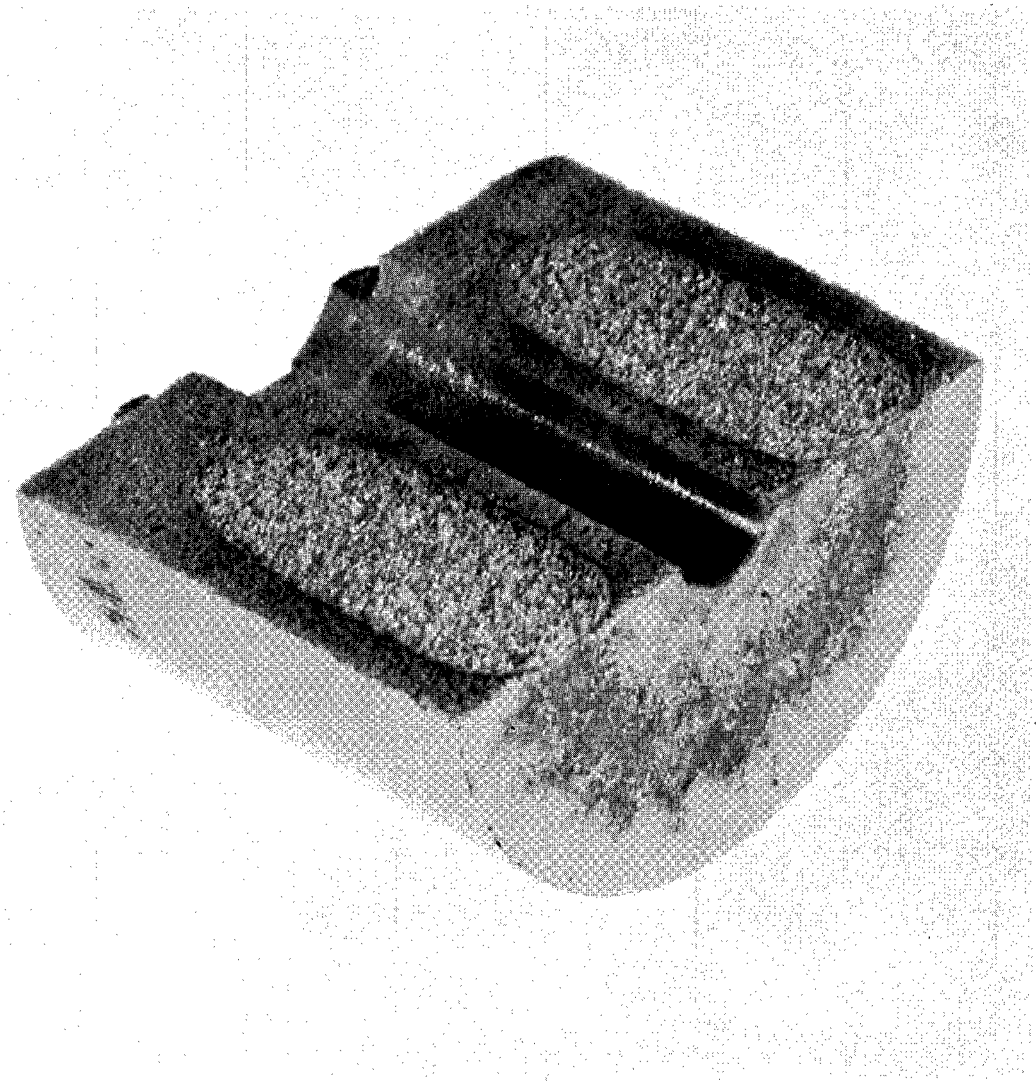

A-38299

Figure 4.- Cut section of plastic sabot.

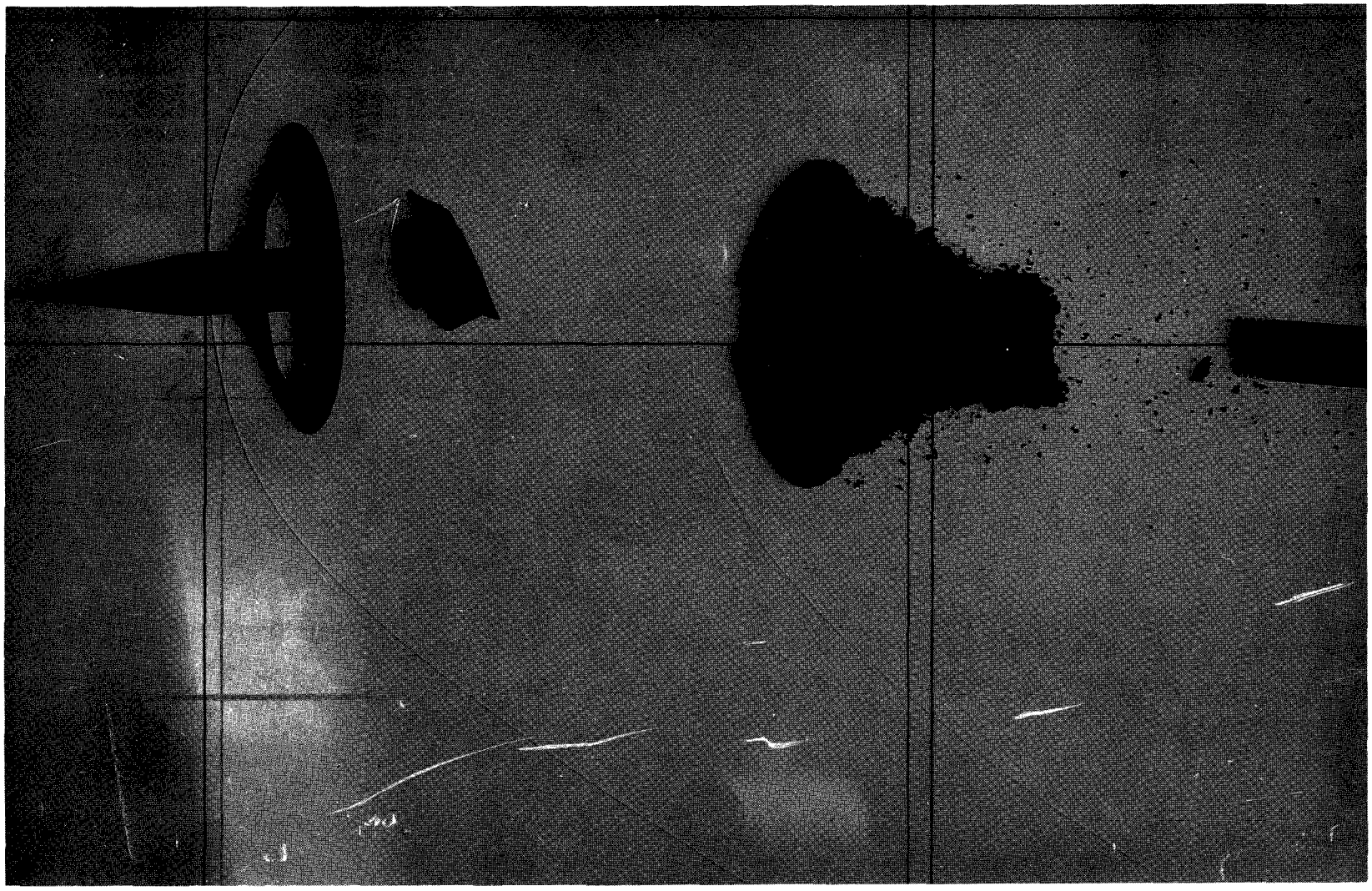

Figure 5.- Shadowgraph of model and sabot separation.

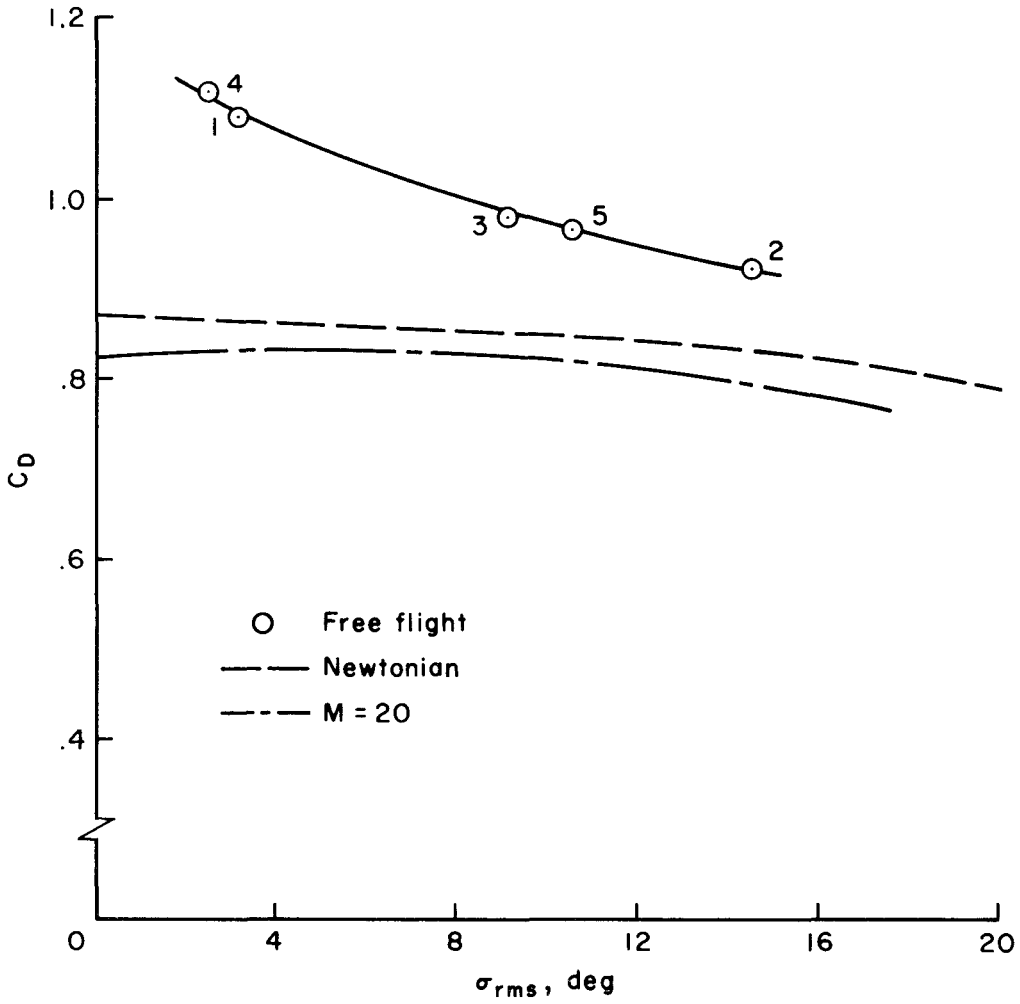

Figure 6.- Drag coefficient vs. root mean square angle of attack.

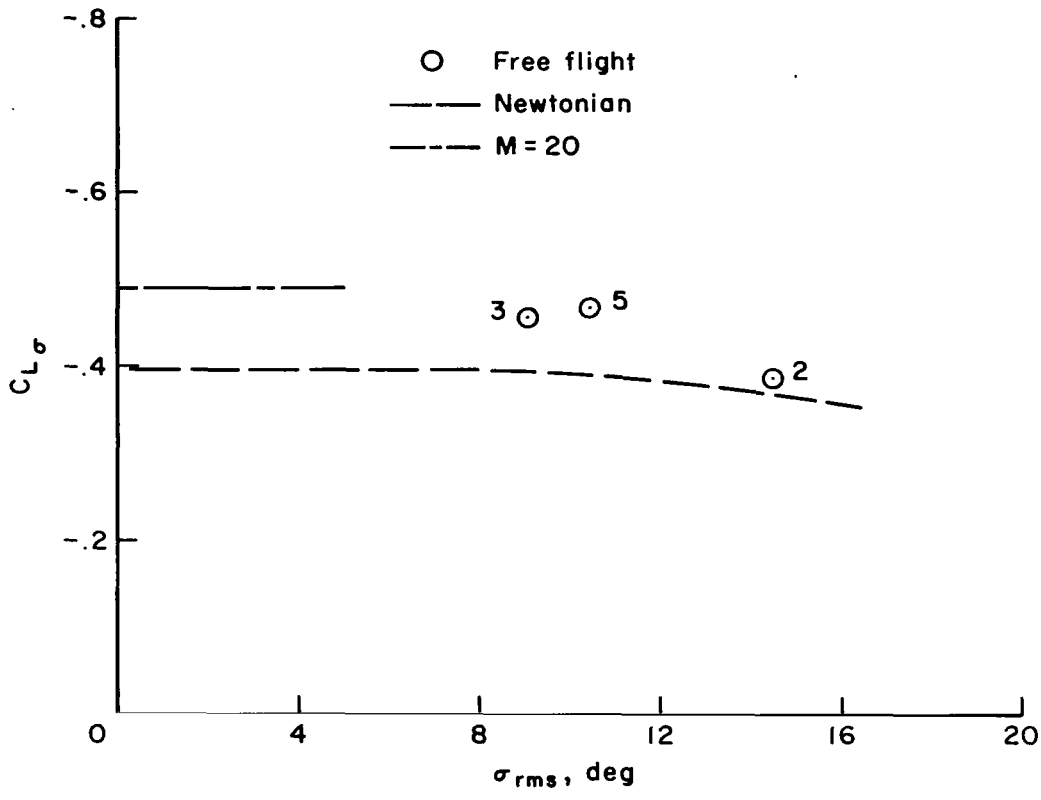

Figure 7.- Lift-curve slope vs. root mean square resultant angle of attack.

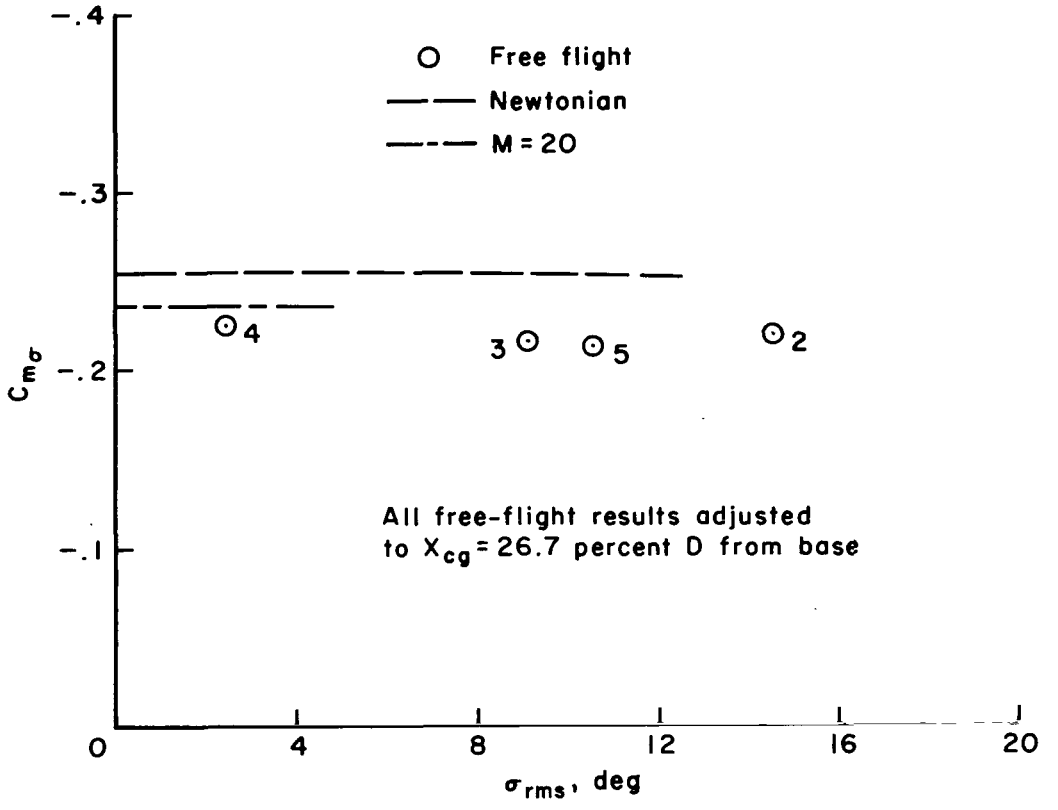

Figure 8.- Pitching-moment-curve slope vs. resultant angle of attack.

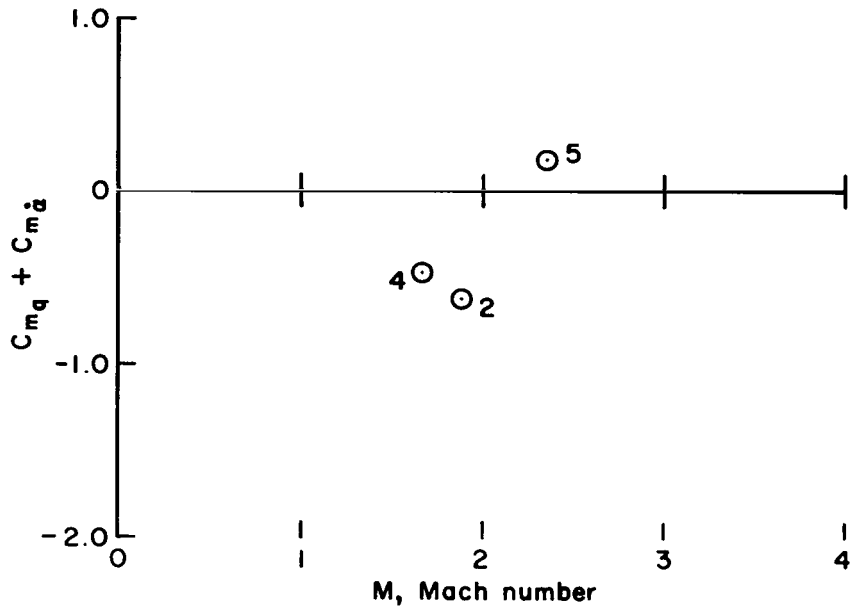

Figure 9.- Damping derivative ($C_{m_q} + C_{m_{\dot{\alpha}}}$) vs. Mach number.

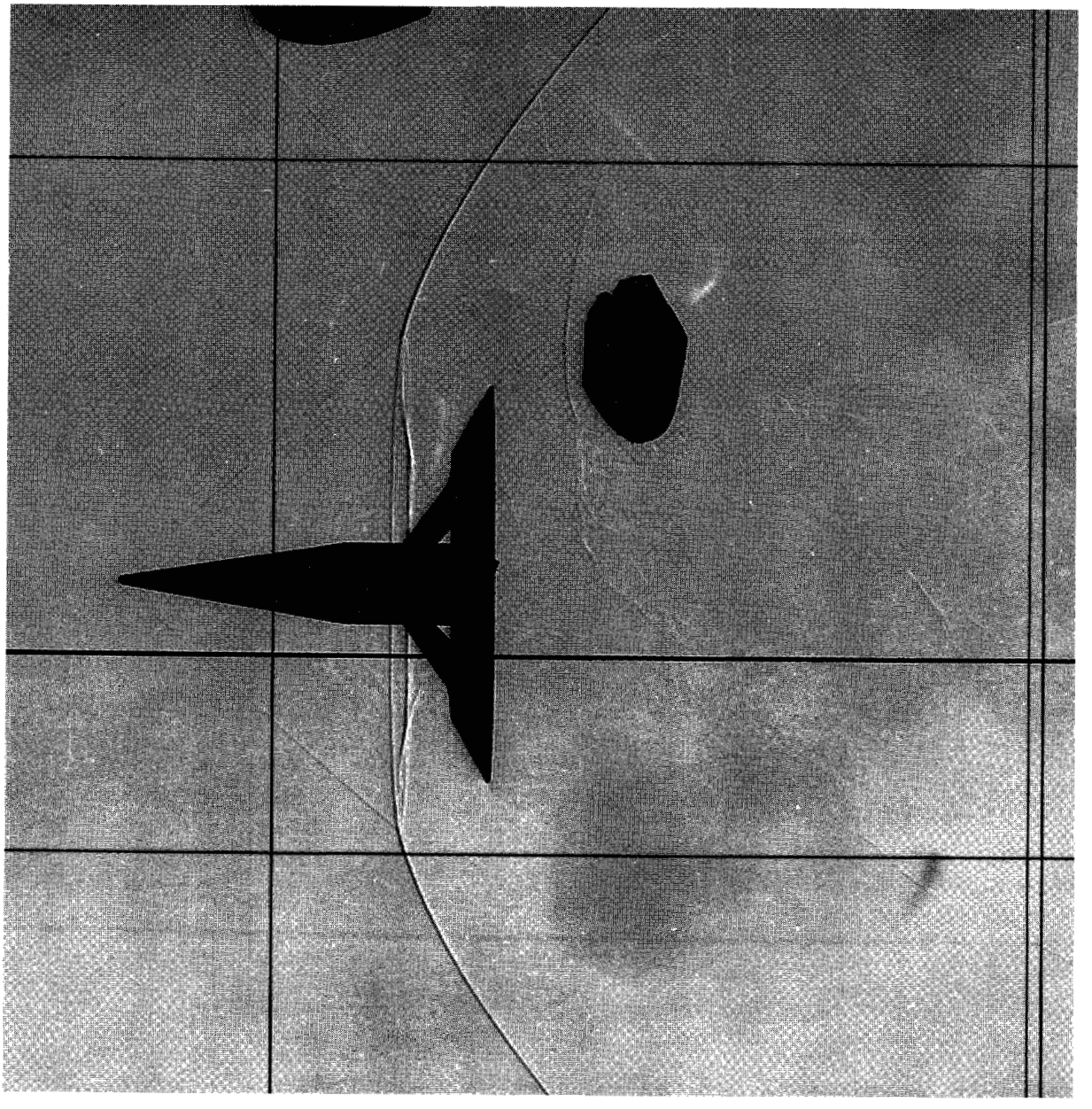

(a) M = 1.901, α = -0.1°, β = -3.5°

Figure 10.- Shadowgraphs of model in flight.

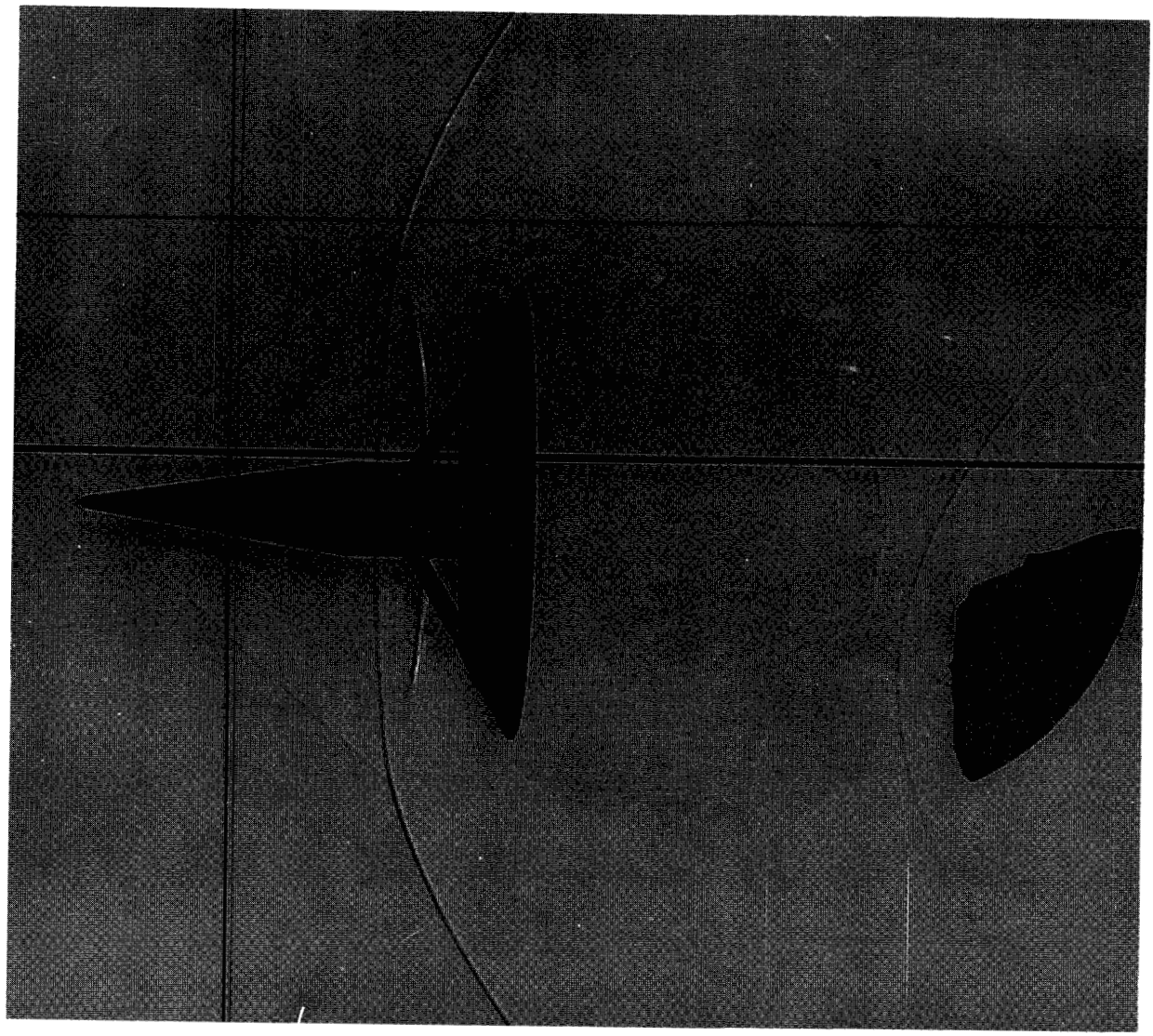

(b) $M = 1.836$, $\alpha = 0.3^{\circ}$, $\beta = -2.93^{\circ}$

Figure 10.- Continued.

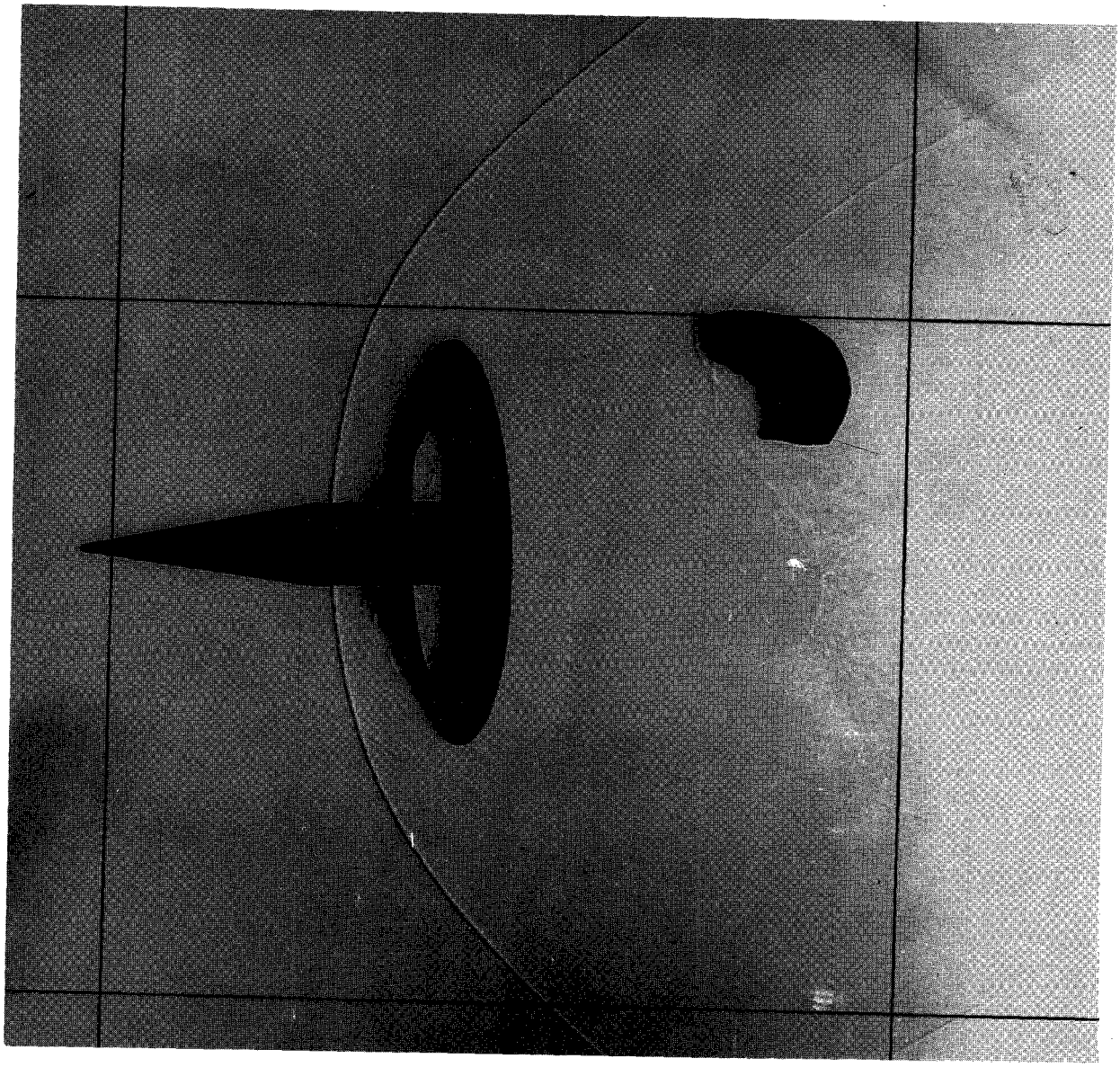

(c) $M = 2.357$, $\alpha = -12.9^{\circ}$, $\beta = -2.5^{\circ}$

Figure 10.- Continued.

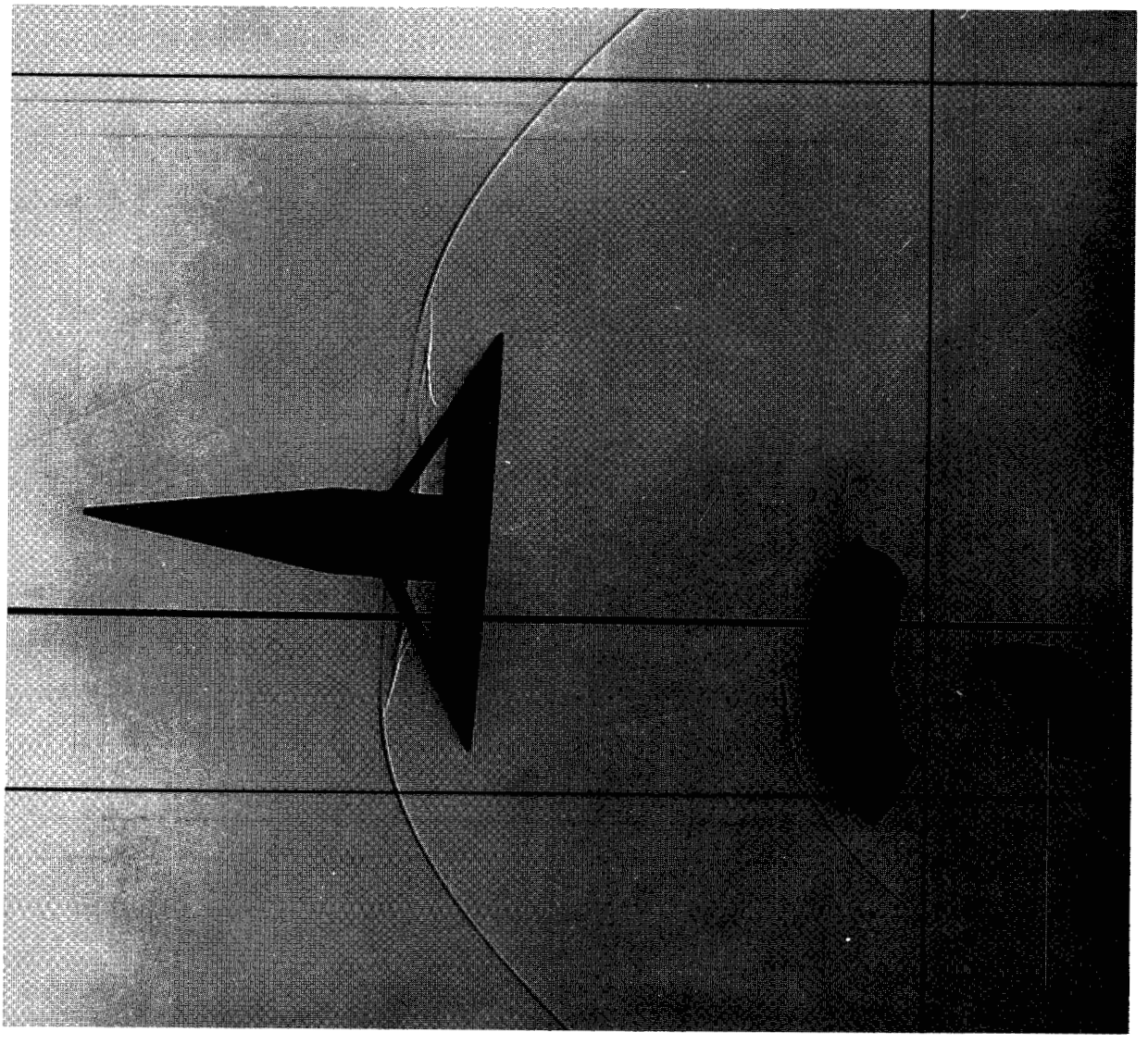

(d) $M = 2.331$, $\alpha = 3.6^{\circ}$, $\beta = 3.5^{\circ}$

Figure 10.- Concluded.

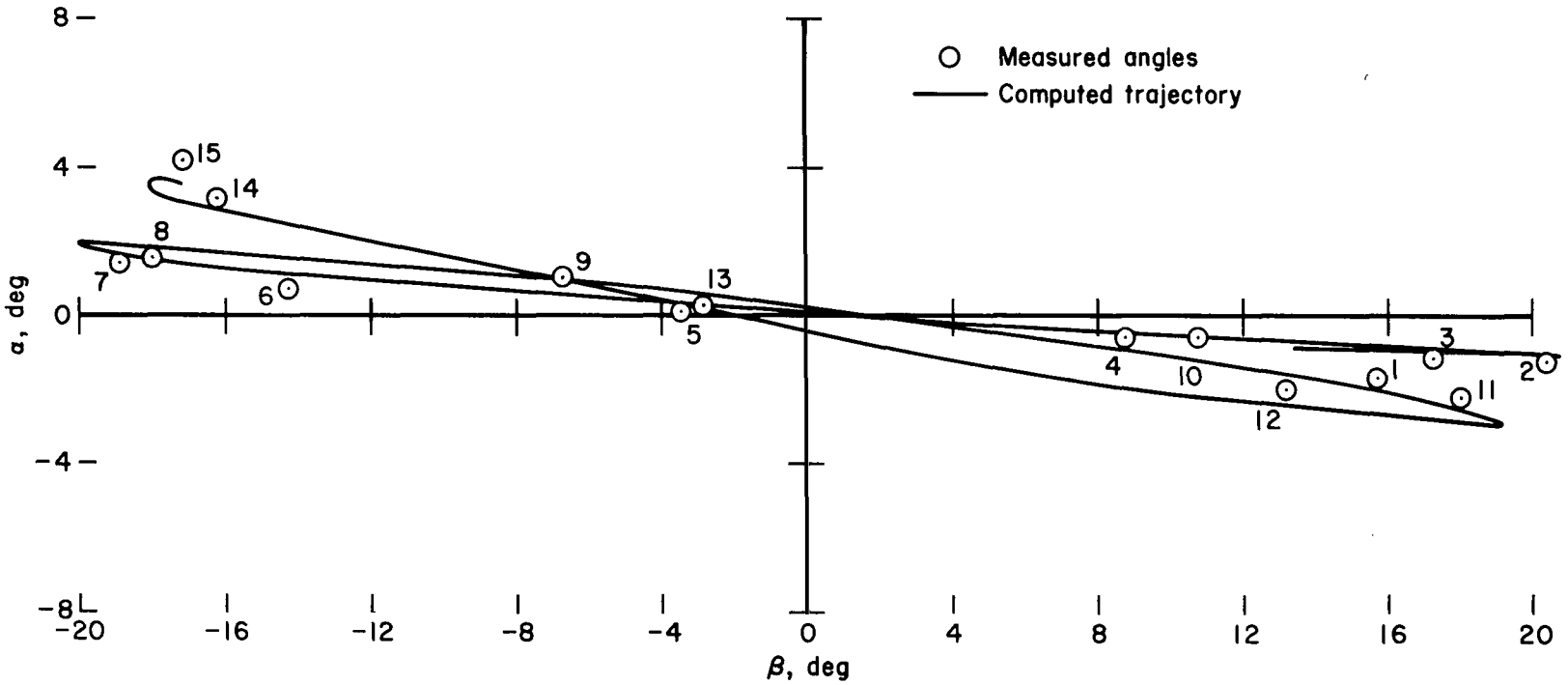

(a) Flight 2, M = 1.874.

Figure 11.- Model flight trajectories and their computed fit.

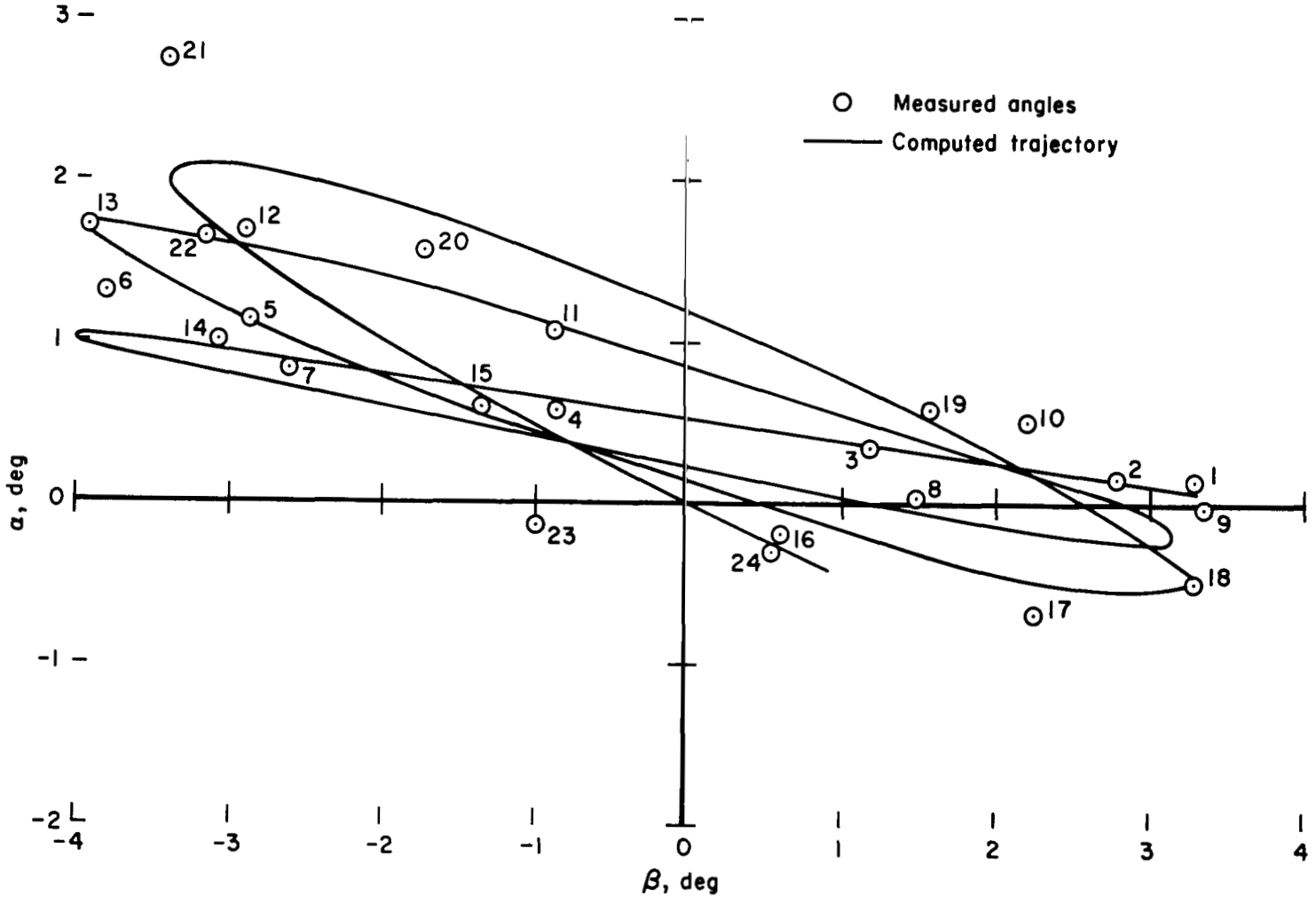

(b) Flight 4, M = 1.638.

Figure 11.- Continued.

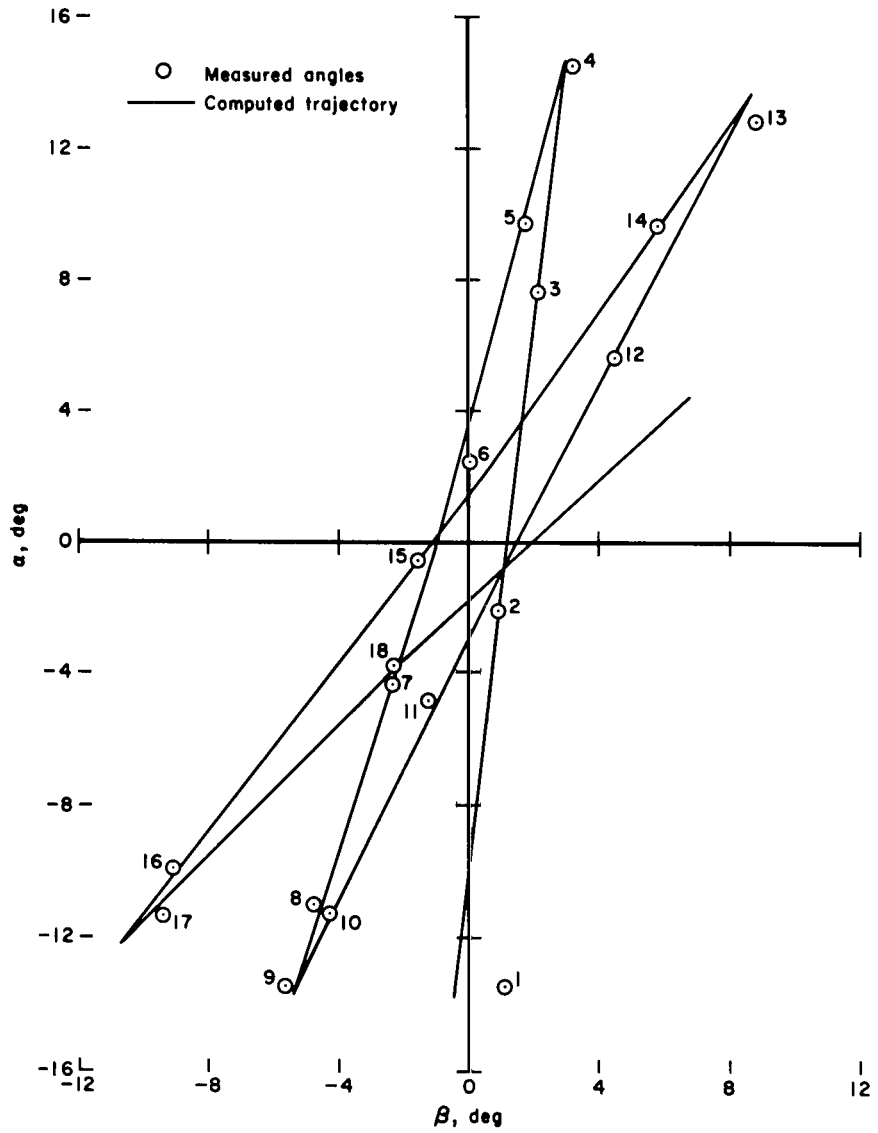

(c) Flight 5, M = 2.358.

Figure 11.- Concluded.

"The aeronautical and space activities of the United States shall be conducted so as to contribute . . . to the expansion of human knowledge of phenomena in the atmosphere and space. The Administration shall provide for the widest practicable and appropriate dissemination of information concerning its activities and the results thereof."

—NATIONAL AERONAUTICS AND SPACE ACT OF 1958

NASA SCIENTIFIC AND TECHNICAL PUBLICATIONS

TECHNICAL REPORTS: Scientific and technical information considered important, complete, and a lasting contribution to existing knowledge.

TECHNICAL NOTES: Information less broad in scope but nevertheless of importance as a contribution to existing knowledge.

TECHNICAL MEMORANDUMS: Information receiving limited distribution because of preliminary data, security classification, or other reasons.

CONTRACTOR REPORTS: Scientific and technical information generated under a NASA contract or grant and considered an important contribution to existing knowledge.

TECHNICAL TRANSLATIONS: Information published in a foreign language considered to merit NASA distribution in English.

SPECIAL PUBLICATIONS: Information derived from or of value to NASA activities. Publications include conference proceedings, monographs, data compilations, handbooks, sourcebooks, and special bibliographies.

TECHNOLOGY UTILIZATION PUBLICATIONS: Information on technology used by NASA that may be of particular interest in commercial and other non-aerospace applications. Publications include Tech Briefs, Technology Utilization Reports and Notes, and Technology Surveys.

Details on the availability of these publications may be obtained from:

SCIENTIFIC AND TECHNICAL INFORMATION DIVISION

NATIONAL AERONAUTICS AND SPACE ADMINISTRATION

Washington, D.C. 20546